

Dynamics of star branched polymers in a matrix of linear chains — a Monte Carlo study

Andrzej Sikorski*^{a)}, Andrzej Kolinski^{a, b)}, Jeffrey Skolnick^{b)}

^{a)} Department of Chemistry, University of Warsaw, PL 02-093 Warsaw, Poland

^{b)} Department of Molecular Biology, The Scripps Research Institute, 10666 N. Torrey Pines Rd., La Jolla, CA 92037, U. S. A.

(Received: January 21, 1994; revised manuscript of March 15, 1994)

SUMMARY:

A simple cubic lattice model of the melt of 3-arm star-branched polymers of various length dissolved in a matrix of long linear chains ($n_1 = 800$ beads) is studied using a dynamic Monte Carlo method. The total polymer volume fraction is equal to 0,5, while the volume fraction of the star polymers is about ten times smaller. The static and dynamic properties of these systems are compared with the corresponding model systems of isolated star-branched polymers and with the melt of linear chains. It has been found that the number of dynamic entanglements for the star polymers with arm length up to 400 segments is too small for the onset of the arm retraction mechanism of polymer relaxation. In this regime dynamics of star-branched polymers is close to the dynamics of linear polymers at corresponding concentration and with equivalent chain length. The entanglement length for star polymers appears to be somewhat larger compared with linear chains.

Introduction

Computer simulations of model polymeric systems have proven to be very useful for understanding the complex dynamics of related physical systems^{1–3)}. Previous work^{2,4,5)} has shown that the effect of entanglement in polymer solutions and melts and its influence on the dynamics of linear and ring polymers is smaller than was originally anticipated based on theoretical considerations^{2,3,6,7)}. The crossover from Rouse-like dynamics in the high friction limit to entangled dynamics at high concentration of long polymers is perhaps located at quite high molecular mass^{2–4)}. This statement is based on theoretical considerations⁸⁾, experiments^{9–11)} and computer simulations^{2,4,12–14)}. In the particular case of polymer chains based on the cubic lattice and consisting of $n_1 = 800$ segments at a volume fraction $\phi = 0,5$ it was shown that in spite of “reptation-like” scaling of the diffusion coefficient $D \sim n^{-2}$, the corresponding scaling of the longest relaxation time and the onset of the crossover regime for the single segment autocorrelation function characterized by the $t^{1/4}$ scaling, the model chains do not reptate^{2–4)}. To the contrary, the lateral diffusion is not suppressed in respect to longitudinal diffusion along a hypothetical tube. The observed scaling of the dynamic properties in this range of molecular weight and polymer density can be satisfactorily explained by a semiquantitative model that does not invoke reptation^{2,15)}. The reason for the constrained dynamics of the model

polymers in these systems comes from few long living entanglement points that act as a large effective friction coefficient superimposed onto the chain fragments that drag the other chains. That can be also shown by careful analysis of the time evolution of a properly defined "primitive path"^{2,4)}. These results do not contradict reptation theory, however, they indicate that for the majority of high density polymer solutions and melts the reptation mechanism of chain disentanglement is perhaps shifted to a much higher degree of polymerization than it was expected initially. What these simulations show is that experimentally observed "reptation like" scaling of dynamic properties does not necessarily indicate the reptation mechanism on the molecular level^{2,16)}. It should be noted that complementary simulations by Kremer and Grest¹³⁾, employing more straightforward Molecular Dynamics technique, lead to a very similar scaling of the single segment and the center of mass autocorrelation functions. For the longest chains, $n > 100$, there was a clear evidence for $t^{1/4}$ type behavior (the fit gives an exponent of $0,28 \pm 0,03$). This is in very good agreement with predictions of the reptation theory and with the previously discussed results of lattice simulations^{2,4,5)} if one takes into account the fact that the model chains in the model of Kremer and Grest correspond to about three times longer chains on the cubic lattice. For the longest chains in the work of Kremer and Grest ($n = 400$) the time of simulation needed to see relaxation of the entire chain is apparently many times too short. It should be noted that the recently proposed fast fluctuating-bond algorithm for melt simulations may allow studies of longer chains at high densities and over time intervals corresponding to longer times of the real systems¹⁴⁾.

Static and dynamics properties of branched polymers employing continuous¹⁷⁾ as well as lattice models^{18,19)} have been studied extensively by computer simulations. Much less work has been done for concentrated solutions and melts of branched polymers¹⁻³⁾. Needs and Edwards¹⁹⁾ performed Monte Carlo simulations of single 3-arm star-branched long chain polymers (on a simple cubic lattice) in a system of fixed obstacles in order to simulate the cage effect. For this system a very good agreement with the expected^{6,20,21)} exponential scaling of the diffusion coefficient and the longest relaxation time with molecular mass has been observed. The microscopic mechanism was consistent with the arm-retraction mode of the chain relaxation as discussed in several theoretical works^{3,6,20)}.

In this study we address the problem of star-branched polymers in a matrix of long linear chains. This is to our best knowledge the first simulation study of relatively long star-branched polymers in a matrix of long linear chains. The possible cage effect was not assumed a priori but it might emerge from entanglements of long linear chains. Among the questions we address in these simulations are the following^{3,7,21)}:

1. Are the star-branched polymers entangled in a way similar to the linear chains?
2. Is "arm retraction" the leading mechanism of chain disentanglement for the polymer length accessible in simulations on contemporary computers?
3. Is the matrix dynamics (of long linear chains) and consequently the dynamics of the entire system affected by the presence of a small but non negligible fraction of star-branched polymers?

Since the system studied here consists of quite long polymers and the simulation time is sufficient to estimate most of the dynamic properties, the above questions can be

answered to a large extent. We studied a weakly branched system — three-arm stars — in order to observe the entanglement effect in the most straightforward way.

Model

The model of polymers confined to a simple cubic lattice and the model of Monte Carlo dynamics is exactly the same as the one employed in the previous simulations of isolated star-branched polymers^{22,23} and in the extensive studies on melts of monodisperse polymers⁴ and on melts composed of chains of two degrees of polymerization²⁴. For this reason we omit here a description of details of the model dynamics since they can be found elsewhere, together with the discussion of the model ergodicity and its correspondence to the real physical systems^{4,22}. For quick reference, let us just briefly note that the model of the dynamics on the simple cubic lattice employs one-bead (two-bond) corner moves, two-bead crankshaft moves, three-bond (two-bead) permutation moves, and two-bond end moves. All these moves are local and are subject to excluded volume and connectivity restraints. The single time unit of the model simulations is defined exactly as before and expires when each chain is subject to (on average) $(n-2) \cdot N$, $(n-3) \cdot N$, $(n-3) \cdot N$, and 2 attempts of each kind of the above listed local micromodifications, respectively. For star polymers there is one additional move that changes the orientation of the branching point^{22,23}. The time scale of the present simulations is somewhat longer than that of the corresponding simulations of polymer melts.

Results and discussion

Simulations were performed for the volume fraction of polymer $\phi = 0,5$. This volume fraction is defined according to the formula $\phi = \phi_s + \phi_l = (N_s \cdot n_s + N_l \cdot n_l)/L^3$, where N_s (N_l) denotes the number of star-branched (linear) chains, n_s (n_l) the total number of beads in one star-branched (linear) chain and L the edge of the Monte Carlo box.

The linear component was always of length $n_l = 800$ beads. The length of an arm of the star-branched polymer m was assumed to be 32, 50, 100 and 400 beads what implies that the total number of segments $n_s = 94, 148, 298$ and 1198 ($n_s = f \cdot (m-1) + 1$, $f = 3$ is the number of arms). The number of star-branched polymers N_s was equal to 4 for all systems under consideration in order to keep the probe concentration considerably lower than the matrix concentration. The number of linear chains N_l was always about 10 times greater in order to obtain $\phi = 0,5$. The edge of the Monte Carlo box L was 40 (L is always greater than $\langle R^2 \rangle / 2$) for all the lengths of chains under consideration (periodic boundary conditions were used). The summary of the parameters of the studied systems are listed in Tab. 1.

The configurations of the entire system under consideration were recorded at various intervals dependent on the chain length. These trajectories were then used for the calculations of static and dynamic properties.

Tab. 1. Summary of the systems

n_s	N_s	n_1	N_1	L
94	4	39	800	40
148	4	39	800	40
298	4	38	800	40
1198	4	34	800	40

Static properties

We calculated the following parameters describing the macromolecular coil of a star: (i) the mean-square center-to-end distance $\langle R^2 \rangle$, (ii) the mean-square radius of gyration of the entire star macromolecule $\langle S^2 \rangle$, and (iii) the hydrodynamic radius $\langle R_H \rangle$. In Tab. 2, a summary of the static properties is given. All the three parameters mentioned above exhibit the expected scaling behaviour: $\langle R^2 \rangle \sim (n_s - 1)^{1.01 \pm 0.01}$ (values after \pm are standard deviations of the regression lines in log-log scale; real errors could be larger), $\langle S^2 \rangle \sim (n_s - 1)^{0.95 \pm 0.02}$, and $\langle R_H \rangle \sim (n_s - 1)^{0.441 \pm 0.006}$. The values of the exponents are close to those in the case of homopolymeric melts of linear chains⁴⁾ where $\langle R^2 \rangle \sim (n_1 - 1)^{0.987}$ (for the linear chain R^2 has the usual meaning of a mean-square end-to-end distance) and $\langle S^2 \rangle \sim (n_1 - 1)^{1.024}$. The ratio $\langle S^2 \rangle / \langle R^2 \rangle$ is in the same range as results for many models of an isolated star-branched polymer²²⁾. The fourth moments $\sigma_R = \langle R^4 \rangle / \langle R^2 \rangle^2$ and $\sigma_S = \langle S^4 \rangle / \langle S^2 \rangle^2$ are slightly higher than those for a single star-branched chain²²⁾ and close to those of linear chains in the melt⁴⁾. The parameter $g = \langle S^2 \rangle_{\text{br}} / \langle S^2 \rangle_1$ ('br' corresponds to branched and 'l' corresponds to linear with same number of segments) is close to that of a single chain^{18, 22)} and to the random flight model chain ($g = (3f - 2)/f^2 = 0,778$). The parameter $g' = \langle R^2 \rangle_{\text{br}} / \langle R^2 \rangle_1$ is considerably lower for all the systems under consideration compared with the simulation results for an isolated star-branched polymer^{18, 22)} and with random flight chain model predictions²⁵⁾ ($g' = 1 + \frac{1}{8}(f - 1)(\ln 2 - 1/4) = 1,166$). Moreover, the ratio is rather reversed: arms of the star macromolecule in the melt are more contracted compared with linear chains in melt. The next parameter $\rho = \langle S^2 \rangle^{1/2} / \langle R_H \rangle$ is especially useful because it does not involve any data concerning linear chains. ρ is slightly smaller than the corresponding results of simulations for isolated star polymer chains^{18, 23)} (the random flight chain model gives $\rho = [(3f - 2)/(f\pi)]^{1/2} [8(2 - f + 2^{1/2}(f - 1)/(3f))] = 1,401$).

In Tab. 2 we also present parameters describing the matrix consisting of linear chains of length $n_1 = 800$ beads. All these results are the same (within a small statistical error) as for the Monte Carlo simulation of the pure homopolymeric melt of linear chains⁴⁾.

Dynamic properties

We studied the center-of-mass motion by means of the autocorrelation function

$$g_{\text{cm}}(t) = \langle [r_{\text{cm}}(t) - r_{\text{cm}}(t = 0)]^2 \rangle \quad (1)$$

where $r_{cm}(t)$ is the center-of-mass vector at time t . Fig. 1 shows the function g_{cm} versus time t in log-log scale for all the lengths of star macromolecules studied. One can observe from Fig. 1 that the scaling behavior of g_{cm} is qualitatively similar to that of the melt of linear chains⁴⁾. For the mean-square displacements of the center-of-mass lower than $\langle S^2 \rangle$, $g_{cm} \sim t^a$ and the exponent a is lower than unity (see Tab. 3). The value of exponent a decreases with increasing length of the chain (the same as for

Tab. 2. Static properties of star-branched and linear polymers in the systems under consideration

n_s	$\langle R^2 \rangle$	$\langle S^2 \rangle$	$\langle S^2 \rangle / \langle R^2 \rangle$	σ_R	σ_S	g	g'	$\langle R_H \rangle$	ρ
94	55,92	22,28	0,398	1,5078	1,1137	0,770	0,951	4,152	1,136
148	91,42	36,51	0,399	1,5189	1,1183	0,793	0,989	5,132	1,176
298	178,8	70,15	0,392	1,5467	1,1246	0,744	0,966	6,842	1,218
1 198	742,0	257,4	0,347	1,6895	1,0623	0,657	1,013	12,82	1,258
799 ^{a)}	1 649	273,7	0,166	1,5434	1,2138	—	—	12,00	1,379

a) This row displays data concerning the properties of the matrix of linear chains of length 799 segments.

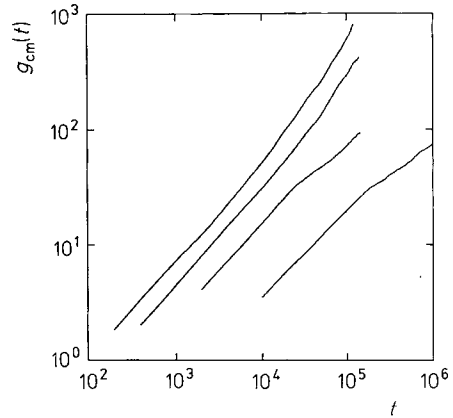


Fig. 1. Log-log plot of the mean-square displacement of the center-of-mass g_{cm} versus time t for various chain lengths ($n_s = 94, 148, 298$ and 1 198 reading from top to bottom)

the linear melt⁴⁾). After a short crossover regime, g_{cm} scales as t^1 . The function g_{cm} calculated for the linear matrix is the same as in the pure linear melt. For the two largest stars, however, the plot does not reach the displacement above the mean radius of gyration. Consequently the obtained estimations for diffusion coefficients have to be treated with some cautions. We discuss this problem below. Deviation of the g_{cm} plot from t^1 scaling may be related to large differences in mobility of particular stars in this range of time reflecting a rather small number of entanglements. A small number of long living entanglements may lead to large relative differences in the degree of constraint of particular stars (and their arms) measured in the time window in the range of the terminal relaxation time. One also cannot exclude a residual contribution to the very slow process of arm retraction.

Tab. 3. Dynamic properties of star-branched and linear polymers in the systems under consideration

n_s	$D \cdot 10^4$	$\tau_R \cdot 10^{-3}$	$10^2 \cdot D\tau_R / \langle R^2 \rangle$	a	$\tau_E \cdot 10^3$	$\tau_a \cdot 10^3$
94	8,86	$1,483 \pm 0,052^d)$	2,35	$0,846 \pm 0,004$	$2,188 \pm 0,042$	$0,612 \pm 0,015$
148	5,25	$4,500 \pm 0,120$	2,58	$0,844 \pm 0,001$	$6,920 \pm 0,066$	$1,948 \pm 0,016$
298	1,57	$24,73 \pm 0,33$	2,17	$0,813 \pm 0,004$	$32,25 \pm 0,44$	$10,92 \pm 0,08$
1 198	$0,152^b)$ $0,095^c)$	579 ± 12	(0,96)	$0,744 \pm 0,003$	663 ± 20	182 ± 8
799 ^{a)}	$0,18^b)$ $0,23^c)$	650 ± 16	(1,25)	$0,696 \pm 0,002$	$1\ 006 \pm 20$	192 ± 3

a) This row displays data concerning the properties of the matrix of linear chains of length 799 segments.

b) Upper bound (see text for details).

c) Lower bound (see text for details).

d) Values after \pm are standard deviations of the regression lines in log-log scale.

The tracer diffusion constant of star branched polymers D_s can be calculated from the function g_{cm} according to Einstein's formula^{2,4)}: $g_{cm} = 6Dt + \text{const}$. In order to omit the initial regime t^a where the motion of the chain is faster, we calculate D_s in the region $2\langle S^2 \rangle < g_{cm} < 10\langle S^2 \rangle$ analogous to the case of a linear polymer melt⁴⁾. Unfortunately, in the case of the longest stars ($n_s = 1\ 198$) a relatively short trajectory does not enable us to extract stable results for g_{cm} in this region. Thus, in this case we calculated the lower bound approximation of D_s assuming that the t^a regime extends to $2\langle S^2 \rangle$. The upper bound approximation was calculated as $g_{cm}/(6t)$ over the appropriate time range (see ref.²⁾ for more details). Values of the diffusion coefficients are collected in Tab. 3.

Fig. 2 shows a log-log plot of the diffusion coefficients D_s versus the total number of segments $n_s - 1$. Values of diffusion coefficients obtained by the same Monte Carlo method for a melt of linear chains²⁾, isolated star-branched polymers²²⁾ and probe linear chains in linear matrices²⁴⁾ are shown in Fig. 2 for comparison. The least-square fit leads to the following scaling formula:

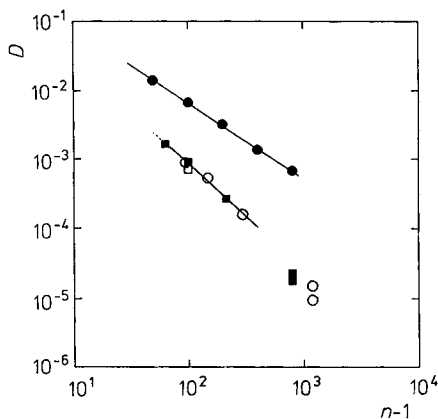
$$D_s \sim (n_s - 1)^{-1,52 \pm 0,15} \quad (2)$$

This exponent was calculated for the first three chain lengths. The tracer diffusion coefficient for the longest chain ($n_s = 1\ 198$) is shown in Fig. 2 (and in Tab. 3) as lower and upper values (see discussion above). Using the mean value of D_s for $n_s = 1\ 198$ and diffusion coefficients for $n_s = 148$ and 298 were obtain the scaling relation

$$D_s \sim (n_s - 1)^{-1,80 \pm 0,03} \quad (3)$$

The exponents in Eqs. (2) and (3) are close to that for a melt of linear chains⁴⁾. The corresponding values for linear chains are 1,53 and 2,04 suggesting the onset of the crossover to the entangled regime with scaling $D \sim N^{-2}$. The ratio of the diffusion coefficients of star polymers to those of linear chains (linear: between 64 and 216 beads,

Fig. 2. Log-log plot of the diffusion coefficients for star-branched polymers in a matrix of linear chains (open circles), isolated star-branched polymers (solid circles), melt of linear polymer (solid squares) and probe linear chain in a matrix of linear chains (open squares) versus the total number of segments. For the longest chains, lower and upper bound of the diffusion coefficient are given. Note: the least-squares fit for the linear melt (dotted line) and for the star-branched polymers in a matrix of linear chains (solid line) are very close



star: between 95 and 299 beads D_s/D_l is equal to 0,98. This ratio is different from that for dilute polymer solutions^{23,26}. In the latter case $D_s/D_l > 1$; this is caused by the smaller dimension (smaller R_{H1}) of star-branched polymers. The ratio obtained in this work $D_s/D_l < 1$ suggests some entanglement effect on the chain dynamics and is in accordance with experimental evidence^{3,21,27,28}.

Needs and Edwards simulations of a star-branched polymer¹⁹⁾ (with $f = 3$ arms) on a simple cubic lattice in the presence of obstacles lead to the conclusion that the diffusion coefficient of a star-branched polymer through fixed obstacles scales as of the following form

$$D_s \sim n_s^{-x} \cdot \exp(-an_s) \quad (4)$$

This scaling is obvious for the star polymer motion through fixed obstacles. Experimental results for the diffusion of star-branched deuterated polybutadiene in the matrix of highly entangled linear polyethylene were interpreted^{3,27,28} to fulfill Eq. (4). On the other hand one can see in Fig. 1 of ref.²¹⁾ that for the degree of polymerization $N < 10^3$ the scaling of the diffusion coefficient can be also considered as consistent with N^{-2} behavior. That is due to the limited accuracy of the experimental data. Some other experimental evidence suggest that in the pure star polymer melt the dependence of the diffusion constant on the chain length is more complex²⁷⁾.

It is possible that the exponential dependence of the diffusion coefficients on the molecular weight would manifest itself for larger chain lengths²⁾. It was suggested that this ratio has to exceed 10 to fulfill Eq. (4). In the case of our simulation the ratio is lower than 10 in all cases (see below). Unfortunately, we could not fit our data to these exponential formulas having results for only four chain lengths.

To obtain a very approximate entanglement length for the model star we used a simple formula of Skolnick, Yaris and Kolinski^{2,4)} to estimate the entanglement length n_c :

$$D = c/(n_s + n_s^2/n_c) \quad (5)$$

where c and n_c are adjustable parameters.

The least-square fit gives $n_e = 160$. This value compared with the total number of segments suggests that only the shortest star-branched polymer ($n_s = 94$) is too short to produce entanglements in melt and the second one ($n_s = 148$) is in the crossover regime. The matrix of linear chains is more entangled (for $n_1 = 800$ the entanglement length could be estimated⁴⁾ as $n_e = 125$).

The autocorrelation function for the single bead

$$g(t) = (1/n_s) \sum_{i=1}^{n_s+1} \langle [r_i(t) - r_i(t=0)]^2 \rangle \quad (6)$$

was also calculated. Fig. 3 shows in a log-log scale the dependence of $g(t)$ on time t for all the chain lengths under consideration. The function $g(t)$ scales as t^1 for the displacements greater than $\langle S^2 \rangle$. The time distance between snapshots on the trajectory is in all cases too large to show the expected^{2,4)} initial scaling $g(t) \sim t^b$ (for short-time, Rouse-like relaxation of the subchains, b is close to 0,5).

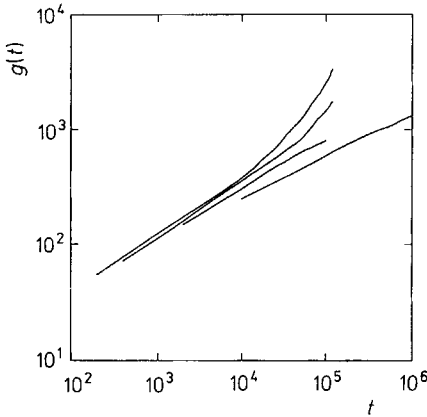
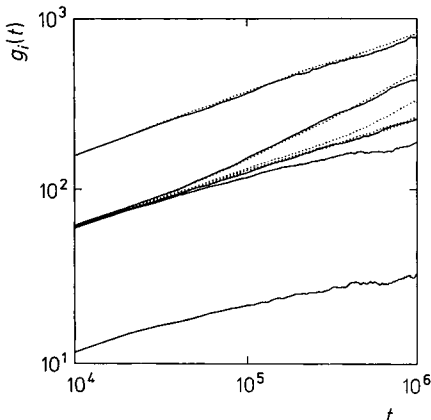


Fig. 3. Log-log plot of the mean-square displacement of the single bead, $g(t)$, versus time t for various chain lengths ($n_s = 94, 148, 298$ and 1198 reading from top to bottom)

Studying the motion of a single bead as a function of the distance from the branching point one can try to answer the question about the possible mechanism of motion of star-branched polymers. Thus, we calculated the mean-square single bead displacement $g_i(t)$ for beads number 1 (the branching point), $m/4$, $m/2$, $3m/4$, m (the end of an arm). This function was averaged over the trajectories and the number of arms. In Fig. 4 we present the functions $g_i(t)$ versus time t in log-log scale for the longest star chain under consideration. For comparison we also plot $g_i(t)$ for the linear chain with $n_1 = 800$ beads. Properties of that chain can be easily compared with the star-branched chain consisting of $n_s = 1198$ beads: one can treat the linear chain as a star with $f = 2$ arms of the same length. One can see that the displacement of a single bead is the same for linear and star chains with the exception of the vicinity of the branching point which moves considerably slower. The slowing down of the mobility of the branching point in comparison to the center of the linear chain is large but it becomes almost negligible for the end portion of the chains. The exponents change from 0,26 (the branching point) through 0,32 ($m/4$, $m/2$ and $3m/4$) to 0,37 (m). The exponent

Fig. 4. Log-log plot of the autocorrelation function of the single bead, $g_i(t)$, depending on the distance from the branching point for the chain $n_s = 198$. Reading from bottom to top are the displacements of bead number: 1, $m/4$, $m/2$, $3m/4$ and m . The dotted lines concern the appropriate $g_i(t)$ of the linear chain $n_l = 800$ (see text for details). Note that there are five dotted lines in the figure: two lines corresponding to the middle part of the chain are very close



0,26 for the branching point is computed for the time window where the data are the most accurate. However, there is some evidence that for longer times $t > 10^5$ the value of the exponent might be considerably smaller. The existence of a $t^{1/4}$ regime is sometimes considered as an evidence for the onset of the reptation mechanism^{2,3}). But this slope of single bead mean-square displacements is found also in systems that cannot reptate⁹).

Coming back to the discussion of possibility of exponential scaling (as given in Eq. (4)) in these model systems, we want to point out that since chain ends relax their conformation much faster than the central core of the model star polymers (as it is illustrated in Fig. 4) it is possible that the weak scaling emerging from the comparison of the data given in Fig. 3 can to a large extent be caused by averaging of the autocorrelation function over the entire molecule. Therefore, the mobility of the outer part of the star polymers might cover the stronger chain lengths dependence governing the motion of the central core. The plots of the branch-point autocorrelation function for various lengths of the arm as shown in Fig. 5 could be helpful. It is clear that there is an increasing width of the "plateau" region with increasing arm length. For the largest stars, it is unclear how wide the plateau is because of the uncertain scaling of $g_i(t)$ versus t for longer times (the exponent may be smaller than 1/4). Consequently, one can not exclude that the model systems are just in the range of the chain lengths (and/or polymer density) prior to the onset of exponential scaling of the dynamic properties^{3,27,28}).

The longest internal relaxation time τ_R , describing the relaxation process of an arm of the star macromolecule^{1,4,22,29}) can be extracted from the center-to-end vector \mathbf{R} autocorrelation function $g_R = \langle \mathbf{R}(t) \cdot \mathbf{R}(t=0) \rangle / \langle R^2 \rangle$. (\mathbf{R} is the vector from the branching point to the end of an arm.) In Fig. 6, representative functions g_R versus time t are plotted in semilogarithmic scale. The behavior of these functions is similar to that in the case of a single star polymer²²) and a melt of linear chains⁴): after a short period of very fast relaxation, g_R fits the equation $g_R \sim \exp(-t/\tau_R)$. The results of the least-squares fits to this equation are shown in Tab. 3.

In order to determine the mechanism of the motion of star-branched polymers in the melt we studied other autocorrelation functions, viz. the function $g_a =$

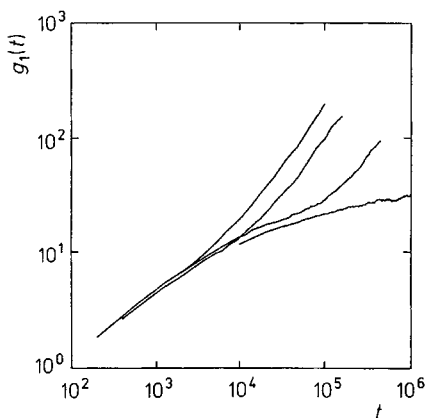


Fig. 5.

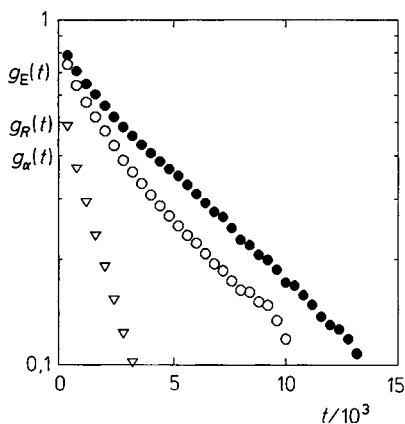


Fig. 6.

Fig. 5. Log-log plot of the autocorrelation function of the branching point g_1 versus time t for various chain lengths ($n_s = 94, 148, 298$ and 1198 reading from left to right)

Fig. 6. Representative semilogarithmic plot of the autocorrelation functions: g_R (open circles), g_E (solid circles) and g_α (open triangles) versus time t for chain $n_s = 148$

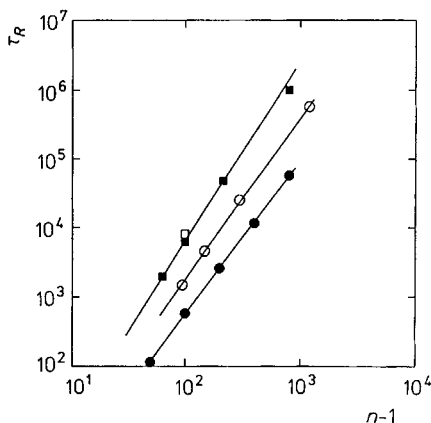


Fig. 7.

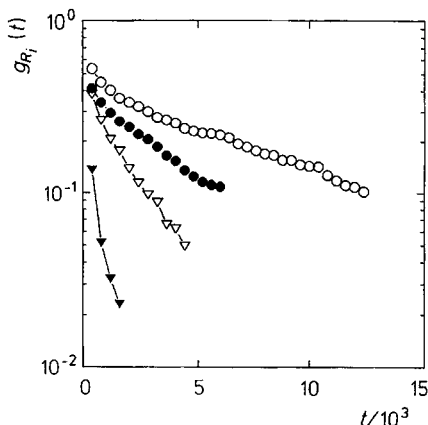


Fig. 8.

Fig. 7. Log-log plot of the longest relaxation times τ_R for star-branched polymers in a matrix of linear chains (open circles), isolated star-branched polymers (solid circles), melt of linear polymer (solid squares) and probe linear chain in a matrix of linear chains (open squares) versus the total number of segments

Fig. 8. Representative semilogarithmic plot of the autocorrelation function g_{R_i} versus time for chain $n_s = 148$. Reading from top to bottom are the g_{R_i} for the subchains between beads: 1 and $m/4$ (open circles), $m/4$ and $m/2$ (solid circles), $m/2$ and $3m/4$ (open triangles), $3m/4$ and m (solid triangles)

$[\langle \alpha(t) \cdot \alpha(t=0) \rangle - \langle \alpha \rangle^2] / [\langle \alpha^2 \rangle - \langle \alpha \rangle^2]$ where α is the angle between a pair of arms in one star polymer chain. This angle is defined as $\langle \mathbf{R}_i \cdot \mathbf{R}_j \rangle / |\mathbf{R}_i| |\mathbf{R}_j|$ where \mathbf{R}_i means the center-to-end vector of the i^{th} arm. Angle α is a scalar and thus we have to apply a different way of calculating the appropriate autocorrelation function. Fig. 6 shows the representative plot of g_α versus time t . One can notice that in the window $0,7 < \ln[g_\alpha] < 0,3$ there is a linear behavior of the function, and thus we can extract the relaxation time of the angle between arms τ_α in the same way as for τ_R (see above). The results of fitting are collected in Tab. 3. The third parameter concerning relaxation we calculated was τ_E — the relaxation time of the end-to-end vector (from the end of an arm to the end of another arm). An example of the appropriate autocorrelation function g_E is presented in Fig. 6 and the results of the least-square fit in Tab. 3.

All the above relaxation times τ_R , τ_α and τ_E exhibit a similar scaling behavior. Fig. 7 shows in log-log scale relaxation times τ_R versus the total number of segments n_s . The least-square fit leads to the following scaling formulas:

$$\tau_R \sim (n_s - 1)^{2,34 \pm 0,03} \tag{7a}$$

$$\tau_\alpha \sim (n_s - 1)^{2,22 \pm 0,03} \tag{7b}$$

$$\tau_E \sim (n_s - 1)^{2,23 \pm 0,04} \tag{7c}$$

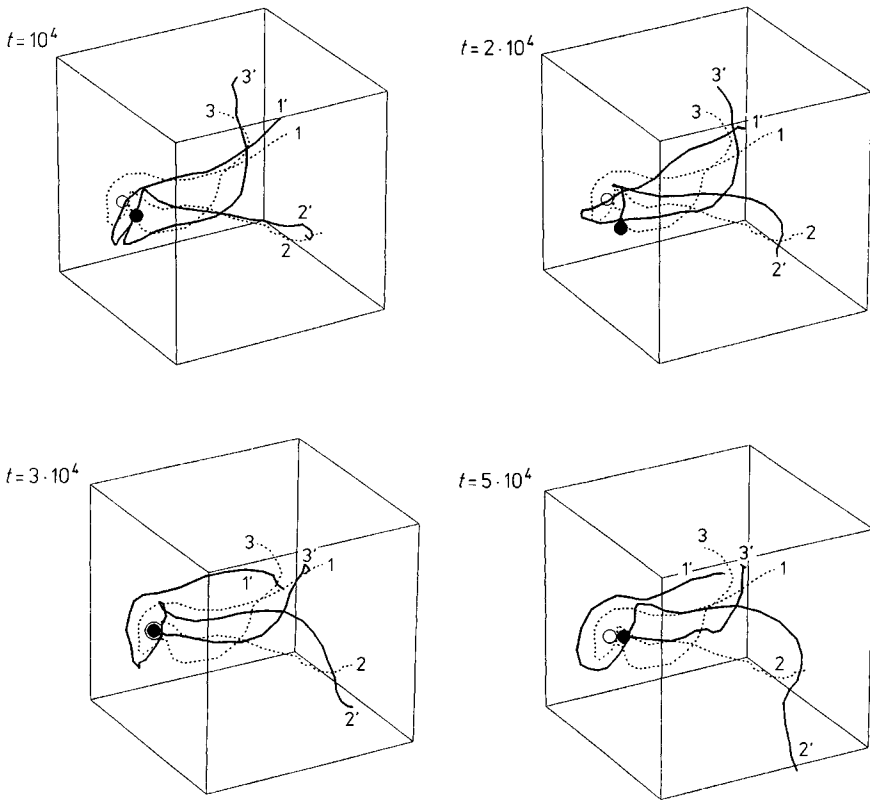
The τ_R exponent can be compared with the Monte Carlo results concerning a melt of linear chains where $\tau_R \sim (n_1 - 1)^{2,63}$ (up to $n_1 = 216$). Fig. 7 shows also the relaxation times of isolated stars and of melts of linear chains.

The relaxation of the angle between arms is $2,4 \div 3$ times faster than the relaxation of the center-to-end vector. The ratio of the relaxation time τ_R to the relaxation time of the end-to-end vector (from the end of an arm to the end of another arm) is approximately constant and close to 1,5. In the case of an isolated star-branched polymer these ratios are $2,7 \div 3,5$ and 1, respectively²³⁾.

This behavior suggests a strong bimodal distribution between “entangled” and “non entangled” arms some of them moving faster, others moving rather slowly. This way the relaxation of the vector \mathbf{R} is controlled by the slowly moving arm. At the same time the angle relaxation is controlled by fast relaxing motions. This may be in accordance with the mechanism of arm retraction.

We also studied the relaxation of subchains of a star’s arm. Every arm was divided into subchains of equal length. The autocorrelation function of the i -th subchain’s end-to-end vector \mathbf{R}_i was calculated. Fig. 8 shows the representative plot of g_{R_i} versus time t for $n_s = 148$ segments. In this case every subchain consisted of $m/4 = 16$ segments. As one can expect the longest relaxation time of a subchain i , τ_{R_i} , increase going from the free end toward the branching point. For the chain $n_s = 148$ these times are: 410 (estimation), 1294, 2365 and 2830. The relaxation time of subchains forming the central core (the closest to the branching point) $\tau_{R_1} = 2830$ is close to τ_R of the entire arm (4500). Consequently (on average) the majority of the dynamic long-living entanglements appears near the branching point.

Using the real configuration of the star-branched polymer we can construct an equivalent primitive path^{2,4)}. Every bead of the original chain was replaced by a point



which corresponds to the center-of-mass of the neighboring (along the arm) n_B beads. This way we can obtain a smooth path of blobs. Fig. 9 illustrates a representative mechanism of a star motion given in several snapshots of the smoothed chain with $n_s = 1198$ (with $n_B = 101$). For short times there are small fluctuations of the arm positions. No preference for lateral versus longitudinal stretching of the arms is seen at this stage. For longer times (up to 10^5 Monte Carlo cycles) there is a clear unwinding of the 1st arm, which has some features of the arm retraction mechanism. However, again the lateral component of the arm motion is not suppressed. Arms 2 and 3 move at the same time quite a distance, without apparent preference for longitudinal versus lateral motion. For long times, the range of the longest relaxation time, the arm number 1 is already in completely different orientation with respect to the rest of the molecule while the two remaining arms to some extent “remember” the initial orientation. This kind of noncoherent relaxation is seen for most of the star (and in various time windows of the trajectory) molecules in the model systems. The picture is consistent with the previously analyzed correlation functions, describing arm relaxation.

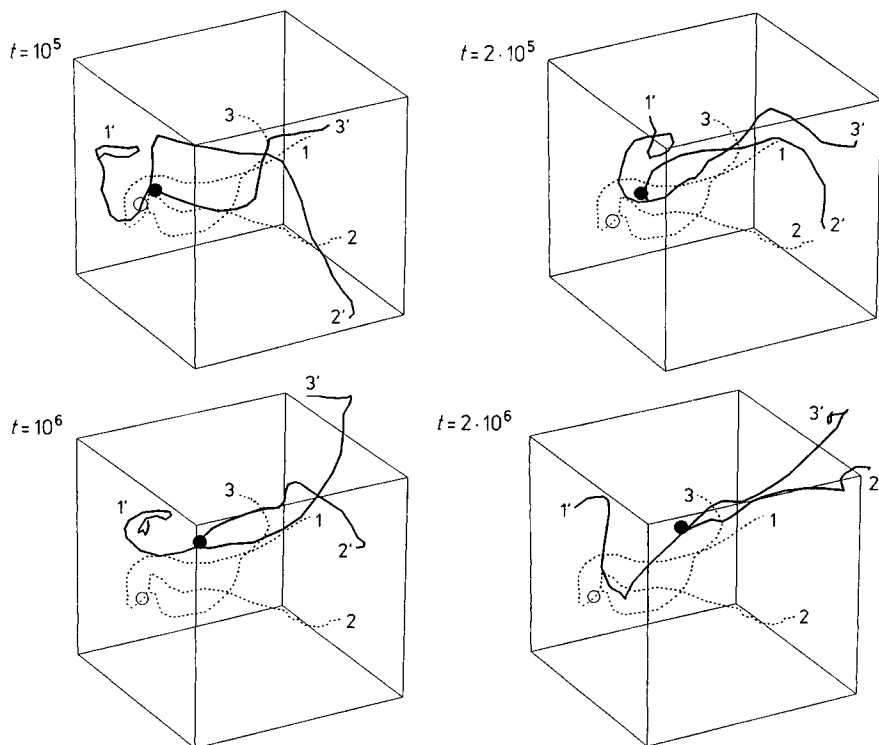


Fig. 9. Snapshot of the primitive path (see the text for the description) of a star-branched chain with $n_s = 1198$ beads. Circles indicate the position of the branching point. Open circles and dashed lines represent the conformation of the star at $t = 0$. The solid lines show the time evolution of the primitive path. For convenience the arms are numbered as 1, 2, 3 at $t = 0$ and 1', 2' and 3' at the given time t

Conclusions

The present work describes simulations of star-branched polymers of various degrees of polymerization (up to relatively high values) dissolved in the matrix of long linear chains. However, even for the longest chains under consideration, $n_s = 1198$ and $n_l = 800$, the entanglement effect seems not to be very strong. The dynamic entanglement length, while larger, for the star-branched polymers is comparable with the entanglement length for linear chains at equivalent conditions⁴⁾. The larger entanglement length of the star polymers can be perhaps explained by a somewhat larger concentration of the segments of the macromolecule within the volume occupied by the star chain⁶⁾. Consequently, the density of other polymers, superimposing topological restraints, has to be smaller. This explanation corresponds very nicely with the much larger entanglement length estimated previously for the melt of long ring (non catenated) polymers^{2, 5, 30)}. For ring polymers the entanglement length (at the same volume fraction) has been estimated to be about three times larger than the entangle-

ment length seen in the melt of linear polymers. Again, the most likely explanation invokes the fact that the ring polymers are more contracted (with $\langle R^2 \rangle \sim n^{0.84}$ and $\langle S^2 \rangle \sim n^{0.87}$, see ref.²⁾ for details), and consequently the density of other molecules has to be smaller in the volume occupied by the test molecule.

The number of dynamic entanglements per one arm of the $n_s = 1198$ star is in the range of 3. In agreement with theoretical predictions^{3,20)} this number is too small for an onset of the arm retraction mechanism of the chain relaxation. Moreover, the relaxation time for the angular correlations between branch (center-to-end) vectors is a few times shorter than the relaxation time of a single arm. This again indicates the absence of the arm retraction mechanism. Additionally, inspection of the motion of particular stars (using animation technique) does not indicate any correlation between the end-to-center distance of an arm and the rate of the motion. On the other hand the observed scaling of the tracer diffusion coefficient and the longest relaxation time for the star polymers is very similar to that observed for previously studied systems of linear polymers⁴⁾ as well as for the matrix chains in the present simulations. This suggests a considerable effect of the topological (fluctuating) constraints on the dynamics of stars.

In conclusion, the star polymers studied here are in the crossover regime where the entanglement effect is strong enough to slow down the dynamics and change the scaling of the dynamic properties from Rouse-like to entangled-like. However, the number of dynamic entanglements is too small to see the arm retraction mechanism and, consequently, the exponential dependence of the diffusion coefficient and the longest relaxation time on the molecular mass. Explicit simulations of the cage effect, as done by Needs and Edwards¹⁹⁾, show a behavior that is consistent with the arm retraction mechanism. Similarly, in the case of linear polymers⁴⁾, the motion in the fixed matrix (where the reptation mechanism is easy to see in simulations) is different from the motion in the unconstrained systems. Perhaps much longer chains have to be simulated in order to see the arm-retraction mechanism in unconstrained systems. Advances in massively parallel computing and new efficient algorithms¹⁴⁾ may allow this in the future.

This research was partially supported by grant no. *BST-439/34/93*. The authors wish to thank Dr. *Piotr Romiszowski* for the helpful discussion and the visualization of the polymer chain motion. We also gratefully acknowledge helpful discussion with Dr. *Artur Baumgärtner*.

¹⁾ A. Baumgärtner, *Annu. Rev. Phys. Chem.* **35**, 419 (1984)

²⁾ J. Skolnick, A. Kolinski, *Adv. Chem. Phys.* **78**, 223 (1990)

³⁾ T. P. Lodge, N. A. Rotstein, S. Prager, *Adv. Chem. Phys.* **79**, 1 (1990)

⁴⁾ A. Kolinski, J. Skolnick, R. Yaris, *J. Chem. Phys.* **86**, 7164 (1987)

⁵⁾ J. Skolnick, A. Kolinski, A. Sikorski, R. Yaris, *Polym. Prepr. (Am. Chem. Soc. Div. Polym. Chem.)* **30**, 79 (1989)

⁶⁾ P. G. de Gennes, "Scaling Concepts in Polymer Physics"; Cornell University Press, Ithaca, NY 1979

- 7) W. W. Graessley, *Adv. Polym. Sci.* **47**, 67 (1982)
- 8) M. Rubinstein, *Phys. Rev. Lett.* **59**, 1946 (1987)
- 9) P. F. Green, P. J. Mills, C. J. Palmstrom, J. W. Mayer, E. J. Kramer, *Phys. Rev. Lett.* **53**, 2145 (1984);
P. F. Green, C. J. Palmstrom, J. W. Mayer, E. J. Kramer, *Macromolecules* **15**, 501 (1985);
P. F. Green, E. J. Kramer, *Macromolecules* **19**, 1108 (1986)
- 10) A. Wesson, I. Noh, T. Kitano, H. Yu, *Macromolecules* **17**, 782 (1984);
H. Kim, T. Chang, J. M. Yohanan, L. Wang, H. Yu, *Macromolecules* **19**, 2737 (1986)
- 11) M. A. Antonietti, J. Coutandin, H. Sillescu, *Macromolecules* **19**, 793 (1986)
- 12) K. E. Evans, S. F. Edwards, *J. Chem. Soc., Faraday Trans. 2*, **77**, 1891, 1921, 1929 (1981)
- 13) K. Kremer, G. S. Grest, *J. Chem. Phys.* **92**, 5057 (1990)
- 14) I. Carmesin, K. Kremer, *Macromolecules* **21**, 2819 (1988)
- 15) J. Skolnick, R. Yaris, A. Kolinski, *J. Chem. Phys.* **86**, 1407 (1988)
- 16) M. Milik, A. Kolinski, J. Skolnick, *J. Chem. Phys.* **93**, 4440 (1990)
- 17) J. J. Freire, J. Pla, A. Rey, R. Prats, *Macromolecules* **19**, 457 (1986);
J. J. Freire, A. Rey, J. G. de la Torre, *Macromolecules* **19**, 457 (1986);
J. J. Freire, A. Rey, J. G. de la Torre, *Macromolecules* **20**, 342 (1987);
J. J. Freire, A. Rey, J. G. de la Torre, *Macromolecules* **20**, 2385 (1987);
B. Smit, A. van der Put, C. J. Peters, J. Arons de Swaan, J. P. J. Michels, *J. Chem. Phys.* **88**, 3372 (1988)
- 18) J. Batoulis, K. Kremer, *Macromolecules* **22**, 4277 (1989);
G. Zifferer, *Makromol. Chem., Theory Simul.* **2**, 319 (1993);
G. Zifferer, *Makromol. Chem., Theory Simul.* **2**, 653 (1993);
A. Sikorski, *Polymer* **34**, 1271 (1993)
- 19) R. J. Needs and S. F. Edwards, *Macromolecules* **16**, 1492 (1983)
- 20) J. Klein, *Macromolecules* **19**, 105 (1986)
- 21) J. Klein, D. Fletcher, L. J. Fetters, *Nature (London)* **304**, 526 (1983)
- 22) A. Sikorski, *Makromol. Chem., Theory Simul.* **2**, 309 (1993)
- 23) A. Sikorski, P. Romiszowski, in preparation
- 24) A. Kolinski, J. Skolnick, R. Yaris, *J. Chem. Phys.* **86**, 7174 (1987)
- 25) A. Miyake, K. F. Freed, *Macromolecules* **16**, 1228 (1983)
- 26) W. Burchard, *Adv. Polym. Sci.* **48**, 1 (1983)
- 27) C. R. Bartels, C. Buckley, Jr., L. J. Fetters, W. W. Graessley, *Macromolecules* **19**, 785 (1986)
- 28) M. Antonietti, H. Sillescu, *Macromolecules* **19**, 798 (1986)
- 29) G. S. Grest, K. Kremer, T. A. Witten, *Macromolecules* **20**, 1376 (1987);
G. S. Grest, K. Kremer, S. T. Milner, T. A. Witten, *Macromolecules* **22**, 1904 (1989)
- 30) A. Kolinski, J. Skolnick, *J. Phys. Chem.* **97**, 3450 (1993)